

## Supporting Information

For

### Design of Off-On Fluorescent Probes for Heavy and Transition Metal ions

Zhaochao Xu,<sup>a,b,c</sup> Su Jung Han,<sup>b</sup> Chongmok Lee,<sup>b</sup> Juyoung Yoon<sup>\*b,d</sup> and David R. Spring<sup>\*a</sup>

<sup>a</sup> Department of Chemistry, University of Cambridge, Lensfield Road, Cambridge, UK. E-mail: [drspring@ch.cam.ac.uk](mailto:drspring@ch.cam.ac.uk)

<sup>b</sup> Department of Chemistry and Nano Science and Department of Bioinspired Science, Ewha Womans University, Seoul, 120-750, Korea, Fax: (+)82-2-3277-3419, E-mail: [jyoon@ewha.ac.kr](mailto:jyoon@ewha.ac.kr)

<sup>c</sup> State Key Laboratory of Fine Chemicals, Dalian University of Technology, Dalian 116012, China

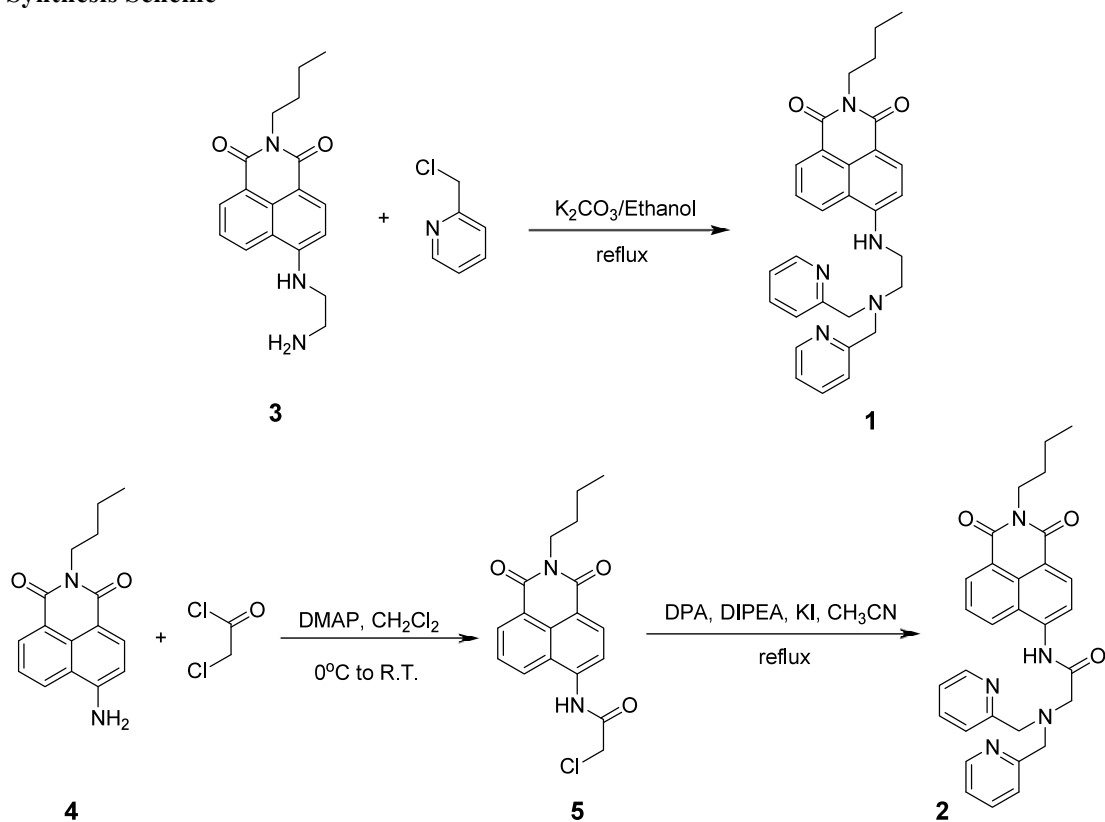
<sup>d</sup> Department of Bioinspired Science, Ewha Womans University, Seoul, 120-750, Korea

#### General methods

Unless otherwise noted, materials were obtained from commercial suppliers and were used without further purification. Flash chromatography was carried out on silica gel 60 (230-400 mesh ASTM; Merck). Thin layer chromatography (TLC) was carried out using Merck 60 F<sub>254</sub> plates with a thickness of 0.25 mm. Preparative TLC was performed using Merck 60 F<sub>254</sub> plates with the thickness of 1 mm.

Melting points were measured using a Büchi 530 melting point apparatus. <sup>1</sup>H NMR and <sup>13</sup>C NMR spectra were recorded using Bruker 250 MHz or Varian 500 MHz. Chemical shifts were given in ppm and coupling constants (*J*) in Hz. UV absorption spectra were obtained on UVIKON 933 Double Beam UV/VIS Spectrometer. Fluorescence emission spectra were obtained using RF-5301/PC Spectrofluorophotometer (Shimadzu).

## Synthesis Scheme



## Syntheses

The synthesis of compound 3 and 4 were according to published procedure.<sup>1,2</sup>

### 4-(bis(pyridin-2-ylmethyl)aminoethyl)amino-*N*-*n*-butyl-1,8-naphthalimide (1):

To a solution of 200 mg (0.64 mmol) *N*-*n*-butyl-4-(aminoethylene)amino-1,8-naphthalimide (3) in 20 mL dry ethanol was added 330 mg (2.6 mmol) picolyl chloride and 300 mg  $K_2CO_3$ . The mixture was then heated at reflux for 10 hours under nitrogen and monitored by TLC. After the reaction was completed, the solvent was removed under reduced pressure. The crude product was then purified by alumina column chromatography ( $CH_2Cl_2$ :MeOH = 100:1) to give (1) as a yellow solid in 65% yield (206 mg). Mp: 165.4-166.9 °C.  $^1H$ -NMR ( $CDCl_3$ , 250 MHz)  $\delta$  0.88 (t,  $J$  = 7.2 Hz, 3H), 1.34-1.43 (m,  $J$  = 7.2 Hz, 2H), 1.57-1.69 (m,  $J$  = 7.2 Hz, 2H), 2.96 (t,  $J$  = 5.0 Hz, 2H), 3.31 (t,  $J$  = 5.0 Hz, 2H), 3.91 (s, 4H), 4.08 (t,  $J$  = 7.2 Hz, 2H), 6.43 (d,  $J$  = 8.4 Hz, 1H), 7.06 (t,  $J$  = 6.2 Hz, 2H), 7.29 (d,  $J$  = 7.5 Hz, 2H), 7.48 (t,  $J$  = 7.5 Hz, 2H), 7.60 (t,  $J$  = 7.8 Hz, 1H), 7.78 (s, 1H, NH), 8.31 (d,  $J$  = 8.5 Hz, 1H), 8.48-8.54 (m,  $J$  = 5.2 Hz, 3H), 8.73 (d,  $J$  = 8.5 Hz, 1H).  $^{13}C$ -NMR ( $CDCl_3$ , 62.5 MHz)  $\delta$  13.92, 20.45, 30.33, 39.91, 40.92, 50.99, 59.69, 103.90, 109.13, 120.74, 122.36, 122.85, 123.30, 124.27, 127.56, 129.99, 130.97, 134.75, 136.66, 149.20, 150.38, 158.73, 164.24, 164.89. HRMS (ESI) calcd for  $C_{30}H_{32}N_5O_2$  [ $MH^+$ ] 494.2556, found 494.2561.

### 4-(2-chloroacetyl)amino-*N*-*n*-butyl-1,8-naphthalimide (5):

A solution of 102 mg (0.9 mmol) of 2-chloroacetyl chloride in 5 ml of dry CH<sub>2</sub>Cl<sub>2</sub> was added dropwise to a solution of 200 mg (0.75 mmol) 4-amino-*N*-*n*-butyl-1,8-naphthalimide (**4**) and 150 mg (1.23 mmol) 4-Dimethylaminopyridine (DMAP) in 30 ml of dry CH<sub>2</sub>Cl<sub>2</sub> stirred in an ice bath. After stirred 2 h at room temperature, the mixture was removed under reduced pressure to obtain a pale-yellow solid, which was purified by silica gel column chromatography using dichloromethane as eluent to afford 4-(2-chloroacetyl)amino-*N*-*n*-butyl-1,8-naphthalimide (**5**). Yield: 221 mg (86%). Mp: 243-244 °C. <sup>1</sup>H-NMR (CDCl<sub>3</sub>, 250 MHz) δ 0.98 (t, *J* = 7.2 Hz, 3H), 1.39-1.48 (m, *J* = 7.2 Hz, 2H), 1.57-1.74 (m, *J* = 7.2 Hz, 2H), 4.16 (t, *J* = 7.2 Hz, 2H), 4.39 (s, 2H), 7.80 (t, *J* = 8.4 Hz, 1H), 8.16 (d, *J* = 8.5 Hz, 1H), 8.45 (d, *J* = 8.0 Hz, 1H), 8.61 (m, 2H), 9.15 (s, 1H, N-H). <sup>13</sup>C-NMR (CDCl<sub>3</sub>, 62.5 MHz) δ 13.86, 20.38, 30.18, 40.31, 43.39, 119.02, 119.65, 123.54, 123.80, 125.66, 127.23, 128.80, 131.34, 132.08, 137.0, 163.45, 163.95, 164.19.

**4-(2-(Di-(2-picolyl)amino)acetyl)amino-*N*-*n*-butyl-1,8-naphthalimide (2):**

4-(2-chloroacetyl)amino-*N*-*n*-butyl-1,8-naphthalimide (**5**) (100 mg, 0.29 mmol), Di-(2-picolyl)amine (DPA) (70 mg, 0.35 mmol), *N,N*-diisopropylethylamine (DIPEA) (0.5 mL) and potassium iodide (30 mg) were added to acetonitrile (50 mL). After stirred and refluxed for 10 h under nitrogen atmosphere, the mixture was cooled to room temperature and the mixture was removed under reduced pressure to obtain a yellow oil, which was purified by silica gel column chromatography (CH<sub>2</sub>Cl<sub>2</sub>:MeOH = 100:1) to afford 4-(2-(Di-(2-picolyl)amino)acetyl)amino-*N*-*n*-butyl-1,8-naphthalimide (**2**). Yield: 124 mg (84%). Mp: 138-139 °C. <sup>1</sup>H-NMR (CDCl<sub>3</sub>, 250 MHz) δ 0.87 (t, *J* = 7.2 Hz, 3H), 1.33-1.39 (m, *J* = 7.2 Hz, 2H), 1.60-1.65 (m, *J* = 7.2 Hz, 2H), 3.55 (s, 2H), 3.98 (s, 4H), 4.07 (t, *J* = 7.2 Hz, 2H), 7.06 (t, *J* = 6.2 Hz, 2H), 7.24 (m, 2H), 7.52 (t, *J* = 7.6 Hz, 2H), 7.74 (t, *J* = 7.8 Hz, 1H), 8.35-8.46 (m, 3H), 8.54 (t, *J* = 8.4 Hz, 2H), 8.98 (d, *J* = 8.4 Hz, 1H), 11.64 (s, 1H). <sup>13</sup>C-NMR (CDCl<sub>3</sub>, 62.5 MHz) δ 13.87, 20.38, 30.19, 40.10, 59.11, 60.57, 116.95, 117.56, 122.69, 122.96, 123.38, 126.20, 128.18, 128.97, 131.01, 132.61, 136.71, 139.78, 149.54, 157.62, 163.70, 164.31, 170.79. HRMS (ESI) calcd for C<sub>30</sub>H<sub>30</sub>N<sub>5</sub>O<sub>3</sub> [MH<sup>+</sup>] 508.2349, found 508.2344.

Reference

1. Liu, B.; Tian, H. *Chem. Commun.* **2005**, 3156-3158.
2. Xu, Z. PhD thesis, Dalian University of Technology (CHN), **2006**.

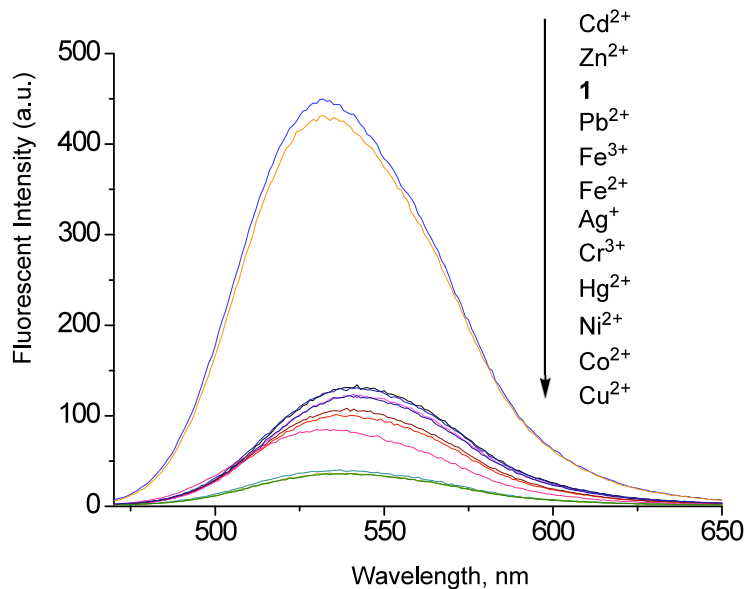


Figure S1. Fluorescence spectra of **1** in the presence of different HTM ions in aqueous solution (CH<sub>3</sub>CN:HEPES = 1:9, HEPES 0.5 M, pH = 7.4). Excitation at 450 nm. [**1**] = 10 μM, [M] = 30 μM.

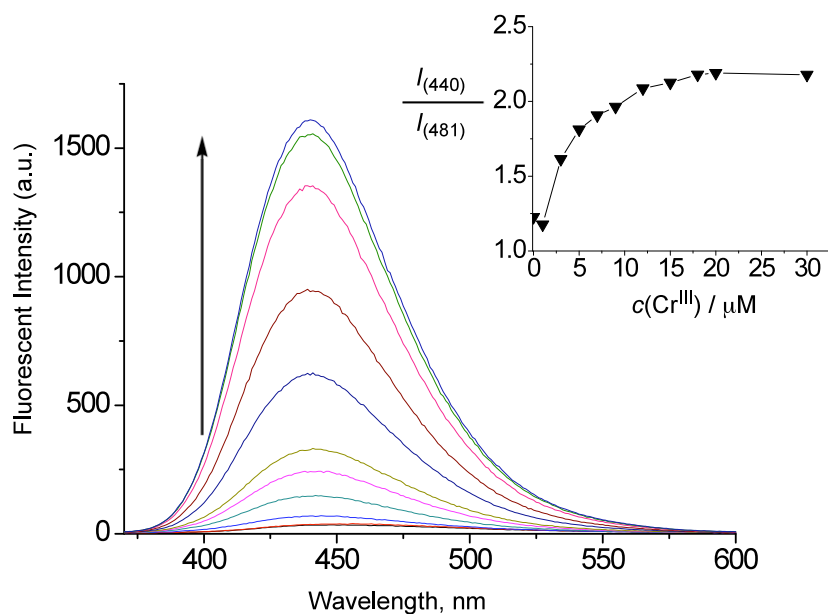


Figure S2. Fluorescence spectra of **2** in the presence of different concentrations of Cr<sup>3+</sup> in CH<sub>3</sub>CN. Excitation at 360 nm. [**2**] = 10 μM. Inset: Ratiometric calibration curve I<sub>440</sub>/I<sub>481</sub> as a function of Cr<sup>3+</sup> concentration.

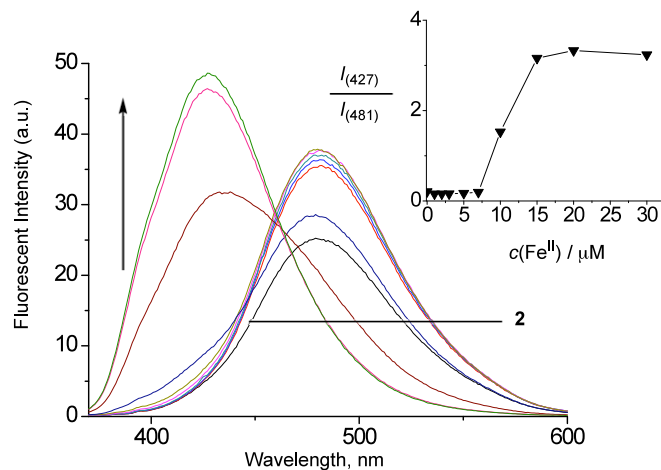


Figure S3. Fluorescence spectra of **2** in the presence of different concentrations of Fe<sup>2+</sup> in CH<sub>3</sub>CN. Excitation at 360 nm. [**2**] = 10  $\mu\text{M}$ . Inset: Ratiometric calibration curve  $I_{427}/I_{481}$  as a function of Fe<sup>2+</sup> concentration.

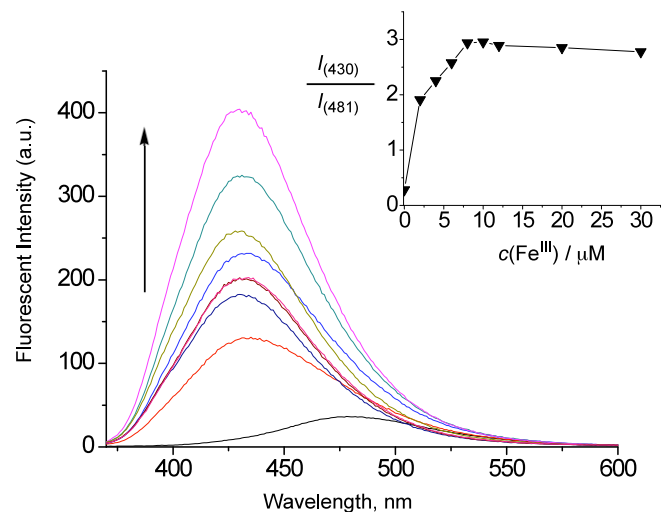


Figure S4. Fluorescence spectra of **2** in the presence of different concentrations of Fe<sup>3+</sup> in CH<sub>3</sub>CN. Excitation at 360 nm. [**2**] = 10  $\mu\text{M}$ . Inset: Ratiometric calibration curve  $I_{430}/I_{481}$  as a function of Fe<sup>3+</sup> concentration.

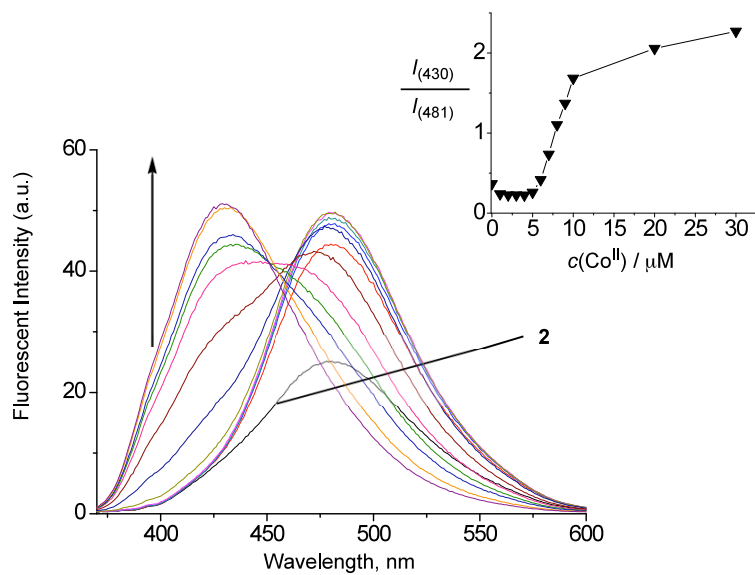


Figure S5. Fluorescence spectra of **2** in the presence of different concentrations of  $\text{Co}^{2+}$  in  $\text{CH}_3\text{CN}$ . Excitation at 360 nm. [**2**] = 10  $\mu\text{M}$ . Inset: Ratiometric calibration curve  $I_{430}/I_{481}$  as a function of  $\text{Co}^{2+}$  concentration.

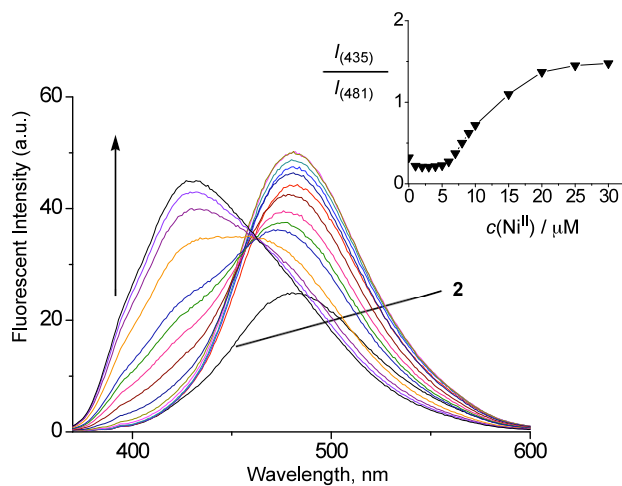


Figure S6. Fluorescence spectra of **2** in the presence of different concentrations of  $\text{Ni}^{2+}$  in  $\text{CH}_3\text{CN}$ . Excitation at 360 nm. [**2**] = 10  $\mu\text{M}$ . Inset: Ratiometric calibration curve  $I_{435}/I_{481}$  as a function of  $\text{Ni}^{2+}$  concentration.

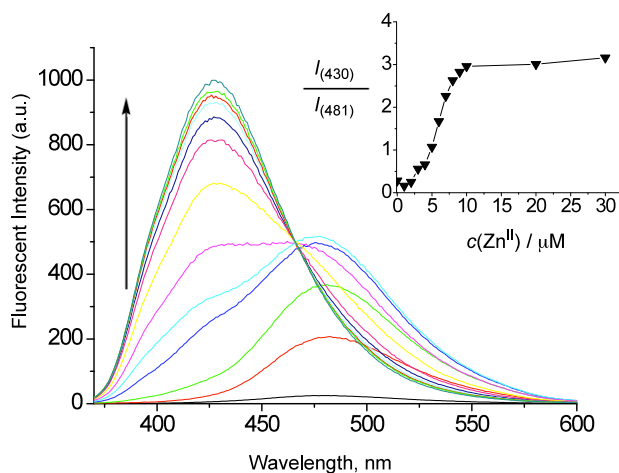


Figure S7. Fluorescence spectra of **2** in the presence of different concentrations of  $\text{Zn}^{2+}$  in  $\text{CH}_3\text{CN}$ . Excitation at 360 nm.  $[\mathbf{2}] = 10 \mu\text{M}$ . Inset: Ratiometric calibration curve  $I_{430}/I_{481}$  as a function of  $\text{Zn}^{2+}$  concentration.

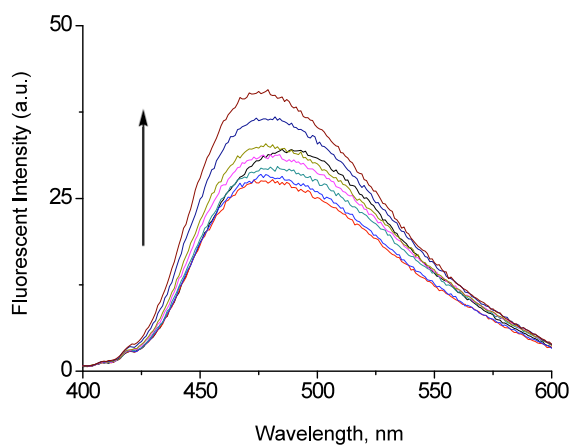


Figure S8. Fluorescence spectra of **2** in the presence of different concentrations of  $\text{Ag}^+$  in  $\text{CH}_3\text{CN}$ . Excitation at 360 nm.  $[\mathbf{2}] = 10 \mu\text{M}$ .

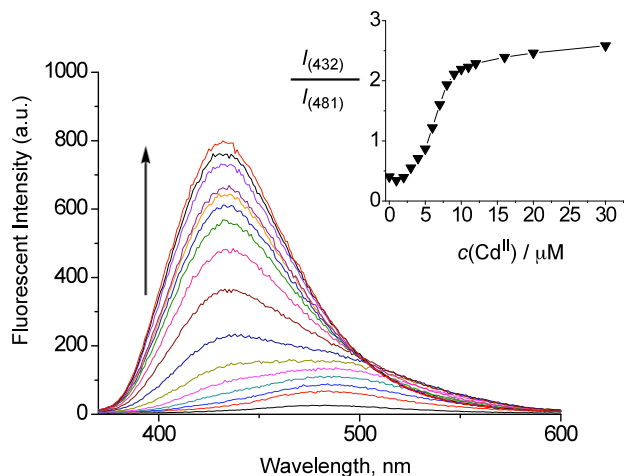


Figure S9. Fluorescence spectra of **2** in the presence of different concentrations of  $\text{Cd}^{2+}$  in  $\text{CH}_3\text{CN}$ . Excitation at 360 nm.  $[\mathbf{2}] = 10 \mu\text{M}$ . Inset: Ratiometric calibration curve  $I_{432}/I_{481}$  as a function of  $\text{Cd}^{2+}$  concentration.

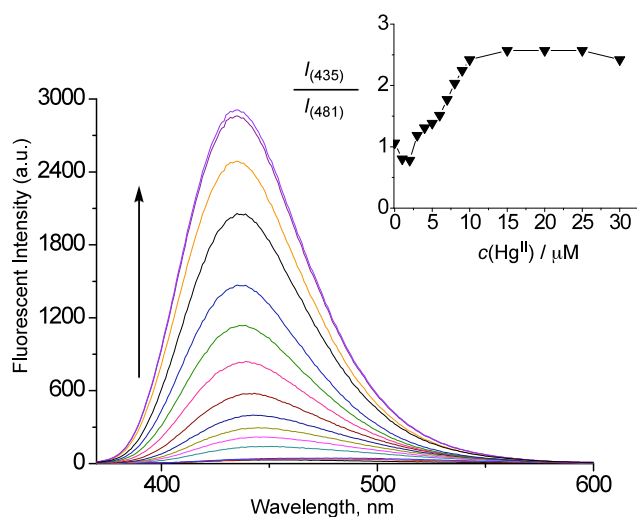


Figure S10. Fluorescence spectra of **2** in the presence of different concentrations of  $\text{Hg}^{2+}$  in  $\text{CH}_3\text{CN}$ . Excitation at 360 nm.  $[\mathbf{2}] = 10 \mu\text{M}$ . Inset: Ratiometric calibration curve  $I_{435}/I_{481}$  as a function of  $\text{Hg}^{2+}$  concentration.

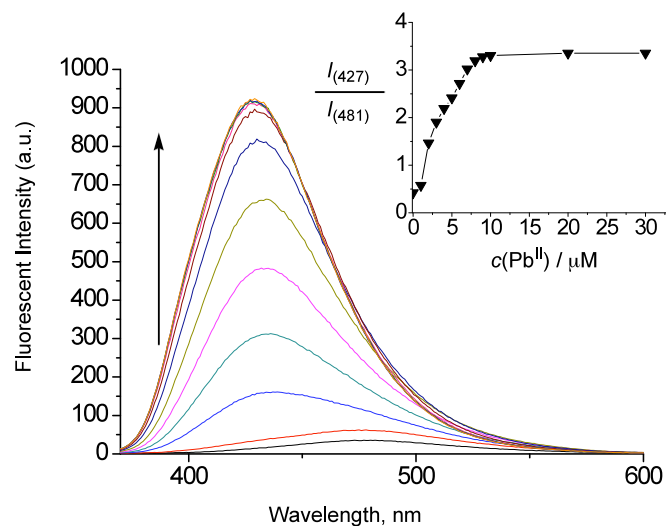


Figure S11. Fluorescence spectra of **2** in the presence of different concentrations of  $\text{Pb}^{2+}$  in  $\text{CH}_3\text{CN}$ . Excitation at 360 nm.  $[\mathbf{2}] = 10 \mu\text{M}$ . Inset: Ratiometric calibration curve  $I_{427}/I_{481}$  as a function of  $\text{Pb}^{2+}$  concentration.

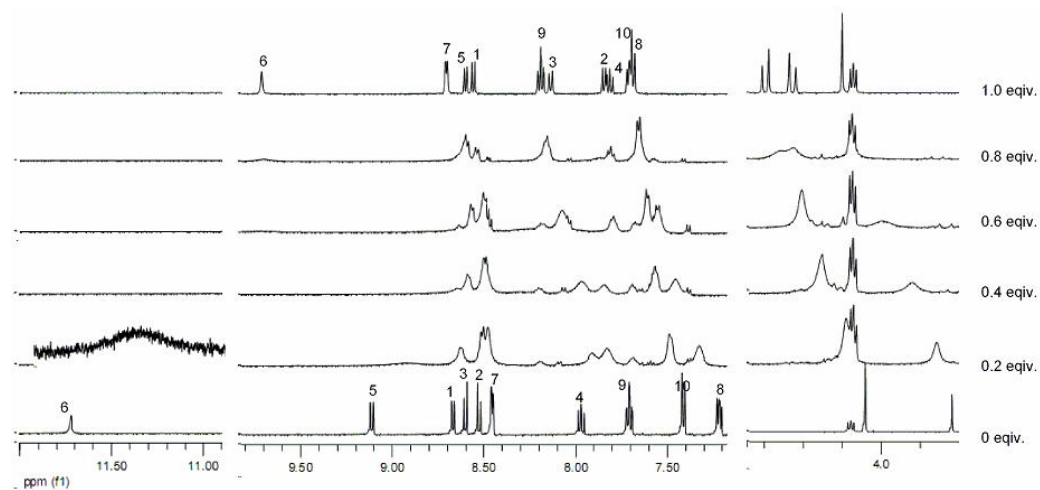


Figure S12.  $^1\text{H}$ -NMR spectra of **2** in the presence of a different amount of  $\text{Zn}^{2+}$  in  $\text{CD}_3\text{CN}$ .

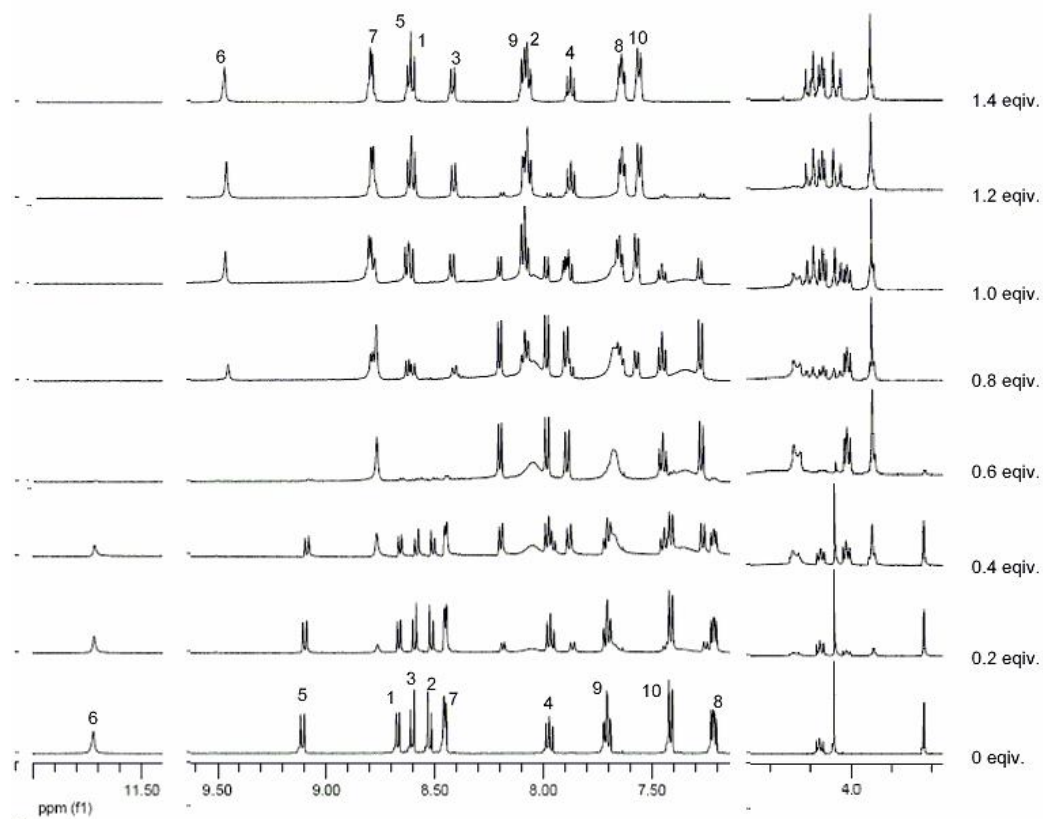


Figure S13.  $^1\text{H-NMR}$  spectra of **2** in the presence of a different amount of  $\text{Cd}^{2+}$  in  $\text{CD}_3\text{CN}$ .

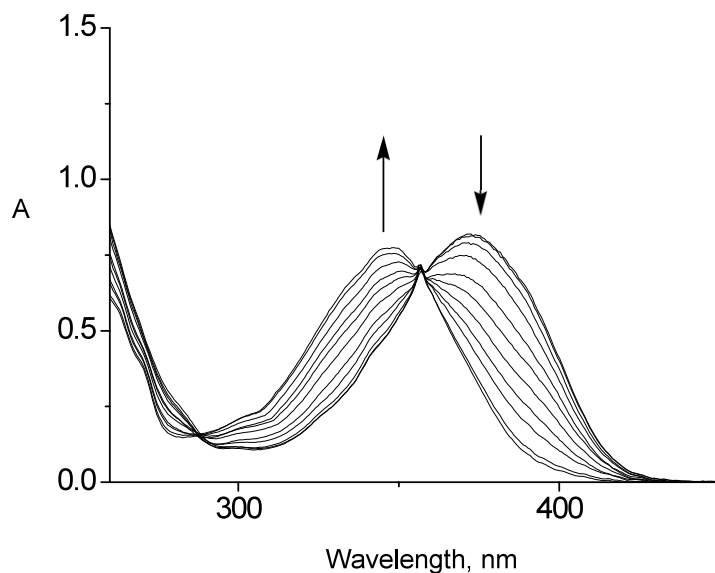


Figure S14. UV-Vis absorption spectra of **2** in the presence of different concentrations of  $\text{Zn}^{2+}$  in acetonitrile.  $[\mathbf{2}] = 10 \mu\text{M}$ ,  $[\text{Zn}^{2+}] = 0\text{-}10 \mu\text{M}$ .

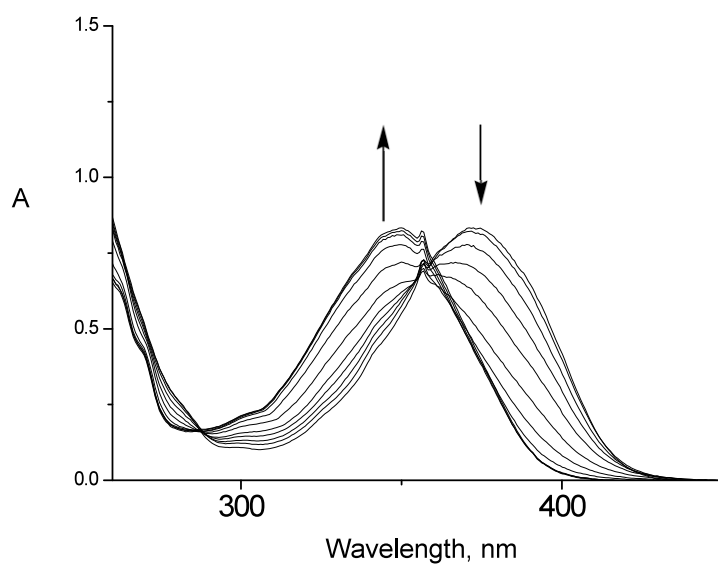


Figure S15. UV-Vis absorption spectra of **2** in the presence of different concentrations of  $\text{Cd}^{2+}$  in acetonitrile.  $[\mathbf{2}] = 10 \mu\text{M}$ ,  $[\text{Cd}^{2+}] = 0\text{-}10 \mu\text{M}$ .

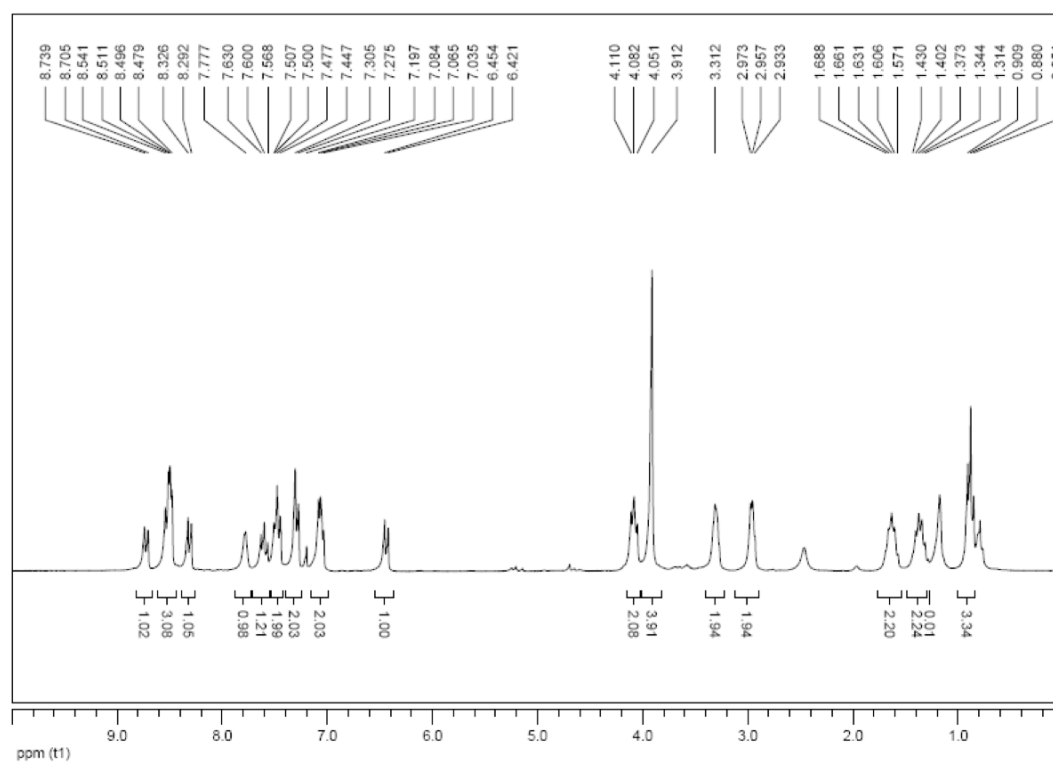


Figure S16.  $^1\text{H-NMR}$  spectra of compound **1** in  $\text{CDCl}_3$ .

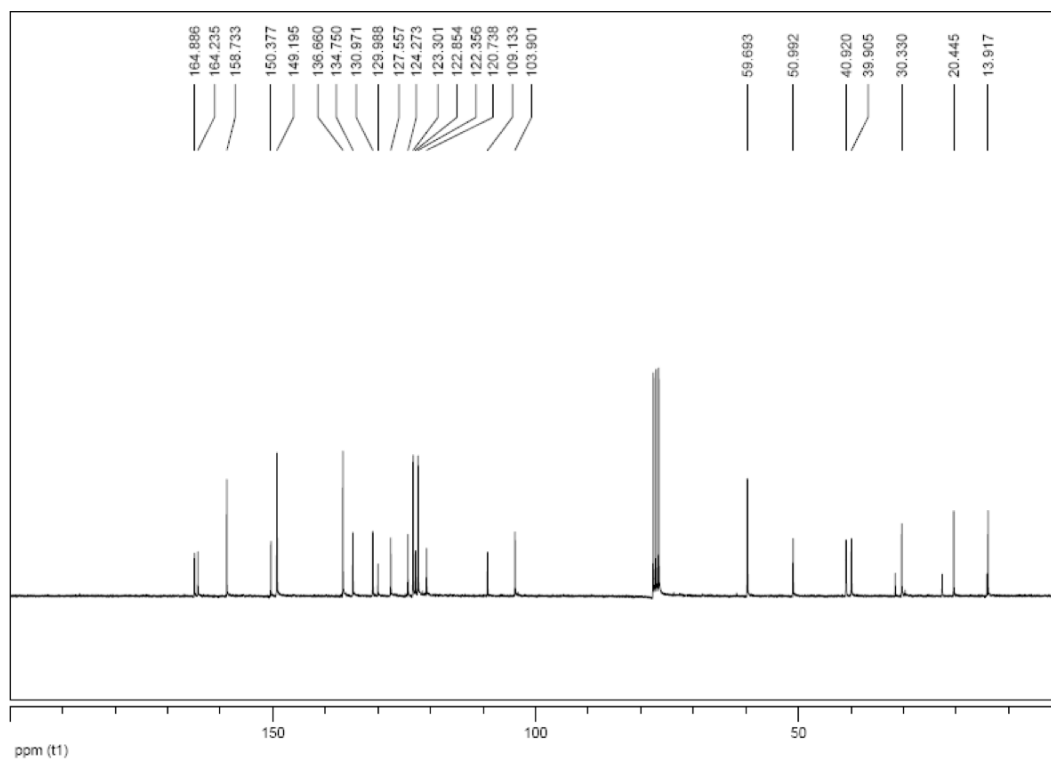


Figure S17.  $^{13}\text{C}$ -NMR spectra of compound **1** in  $\text{CDCl}_3$ .

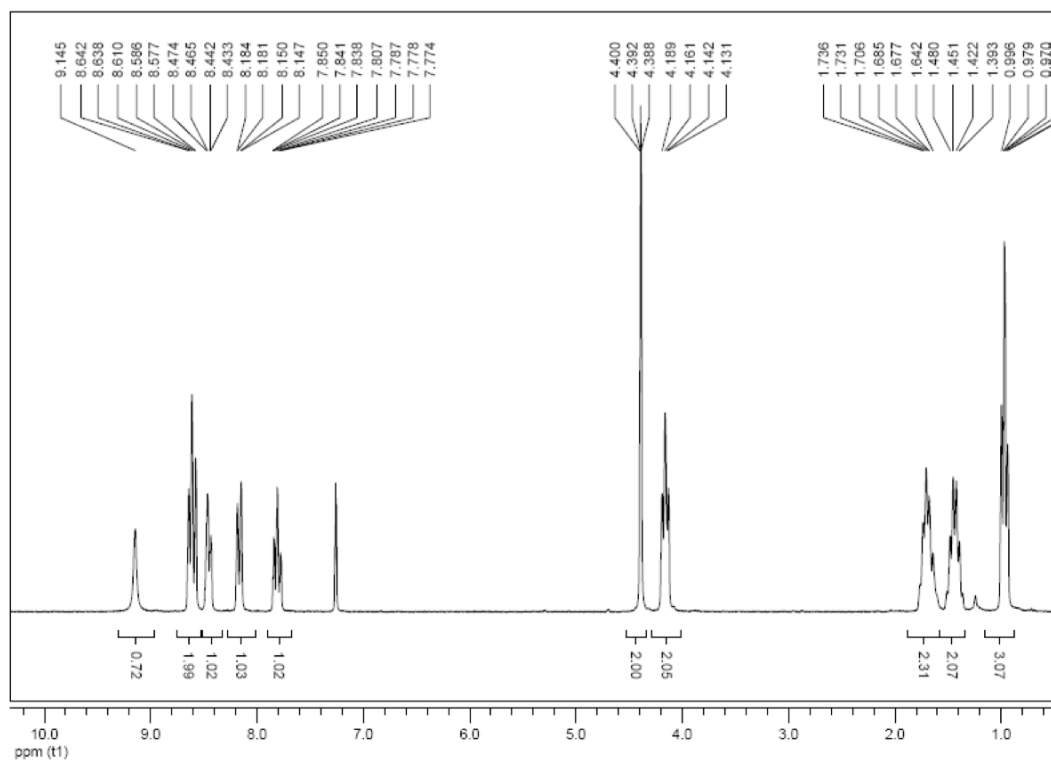


Figure S18.  $^1\text{H}$ -NMR spectra of compound **5** in  $\text{CDCl}_3$ .

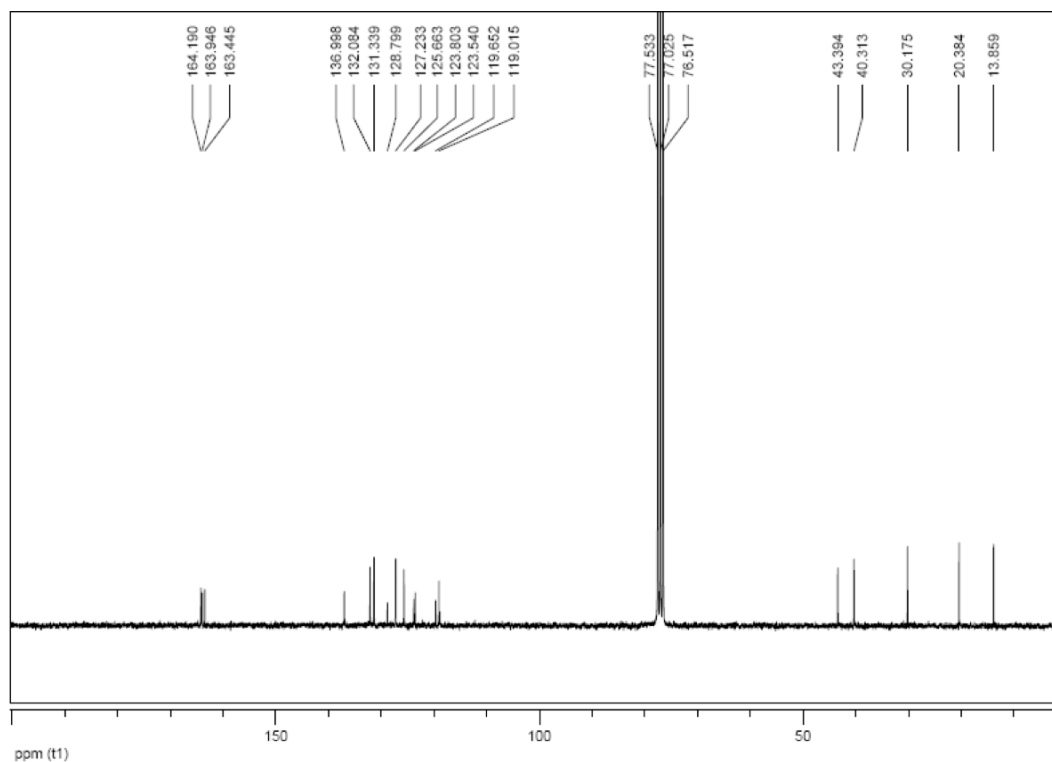


Figure S19.  $^{13}\text{C}$ -NMR spectra of compound **5** in  $\text{CDCl}_3$ .

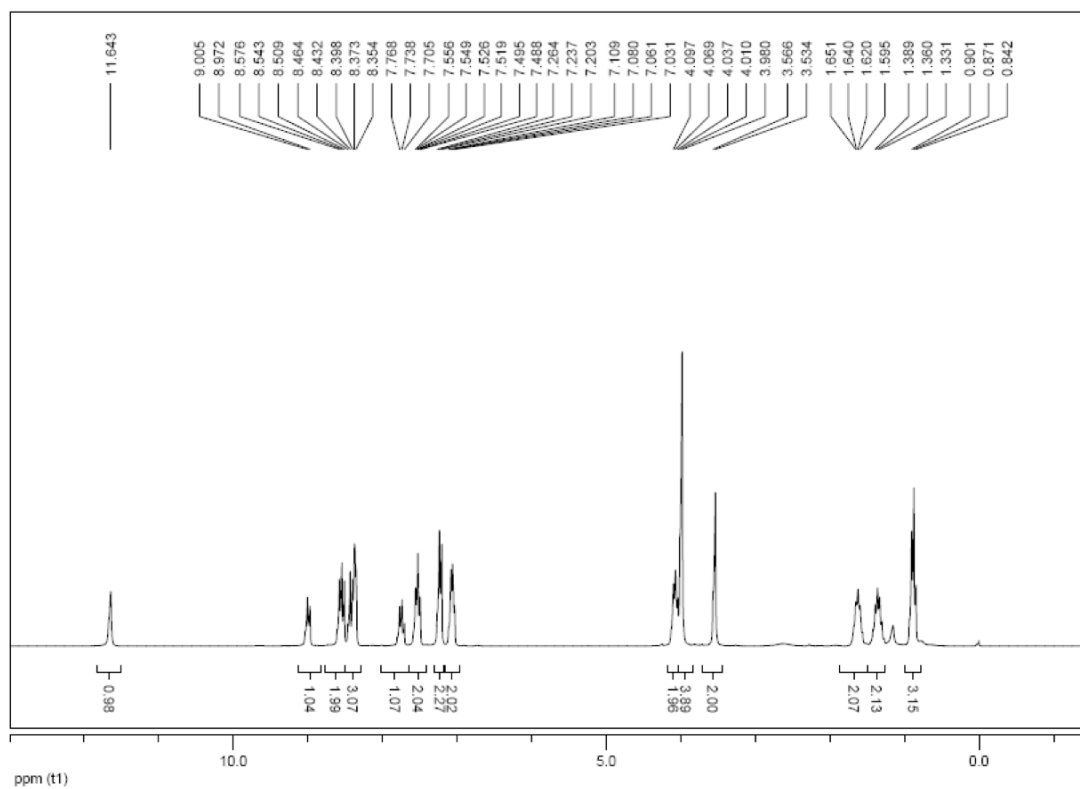


Figure S20.  $^1\text{H}$ -NMR spectra of compound **2** in  $\text{CDCl}_3$ .

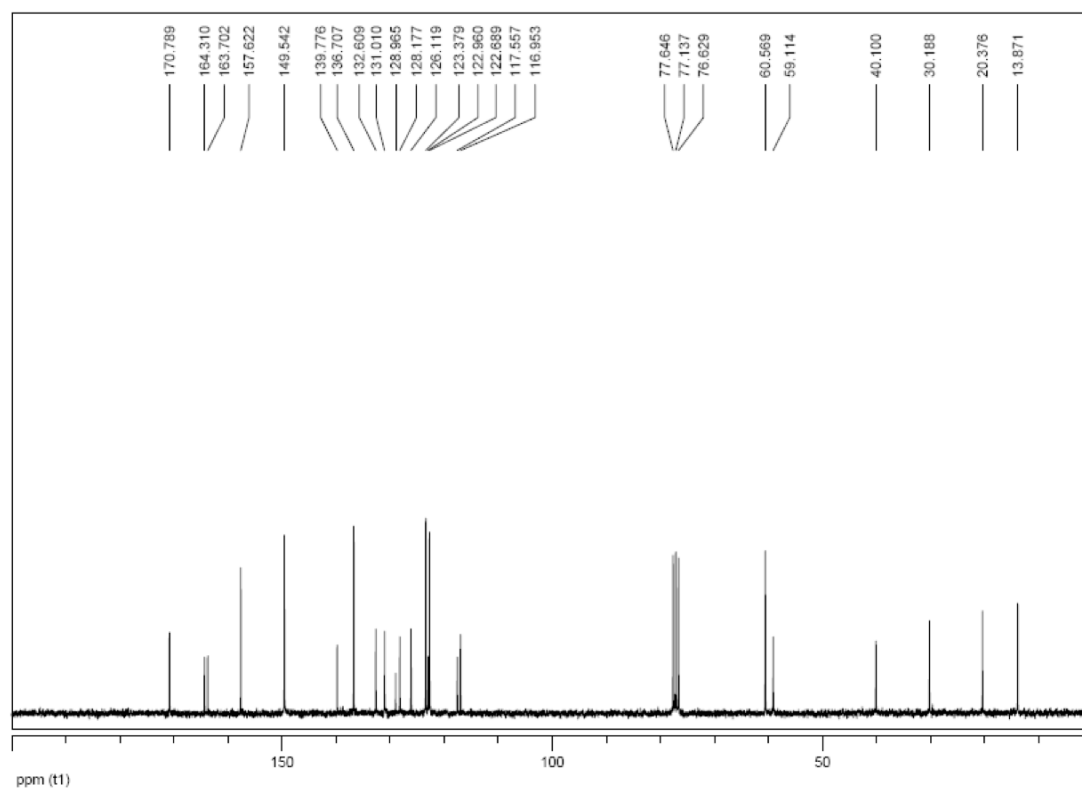


Figure S21.  $^{13}\text{C}$ -NMR spectra of compound **2** in  $\text{CDCl}_3$ .